MONOCLONAL ANTIBODIES IN IMMUNODIAGNOSIS AND IMMUNOTHERAPY
Volume 41, Number 2, 2022

DOI: 10.1089/mab.2021.0048

A Defucosylated Mouse Anti-CD10 Monoclonal Antibody (31-mG_{2a}-f) Exerts Antitumor Activity in a Mouse Xenograft Model of CD10-Overexpressed Tumors

Hiroki Kawabata,[1] Hiroyuki Suzuki,[2] Tomokazu Ohishi,[3] Manabu Kawada,[3] Mika K. Kaneko,[1] and Yukinari Kato[1,2]

CD10 is a glycosylated transmembrane protein and is known as a membrane endopeptidase. It is expressed on predifferentiated lymphocyte progenitor, epithelial, stromal, and tumor cells. Therefore, antibodies against CD10 are used for diagnosing follicular lymphoma and solid tumors, including renal carcinomas. In this study, we developed an anti-human CD10 monoclonal antibody, clone C_{10}Mab-31 (IgG_1, kappa), which detects CD10 by flow cytometry and shows high affinity for CD10-overexpressed CHO-K1 (CHO/CD10) cells. Furthermore, the defucosylated mouse IgG_{2a} version of C_{10}Mab-31 (31-mG_{2a}-f) exhibits antibody-dependent cellular cytotoxicity, complement-dependent cytotoxicity, and antitumor activities in mouse xenografts of CHO/CD10 cells. These results indicate that 31-mG_{2a}-f exerts antitumor effects against CD10-expressing tumors and could be valuable as part of an antibody treatment regimen for them.

Keywords: CD10, monoclonal antibody, ADCC, CDC, antitumor activity

Introduction

CD10 is a type II transmembrane glycoprotein and has been identified as a common acute lymphoblastic leukemia antigen.[1–3] It is expressed on predifferentiated lymphocyte progenitor cells, and is detected on activated and proliferating B cells in the germinal center[4] and on bone marrow stromal cells and neutrophils.[5] CD10 is also expressed in human B-cell malignancies, including follicular,[6] Burkitt, and lymphoblastic lymphomas.[7] Therefore, antibodies against CD10 are used for the diagnosis of follicular lymphoma.[6] Moreover, CD10 is expressed in normal epithelial tissues, including the small intestine, kidney, and lung.

A growing number of evidence suggests that elevated CD10 expression is associated with the malignant progression of several solid tumors.[8] For example, CD10 overexpression has been associated with colorectal cancer development and progression.[9] Furthermore, a direct correlation between CD10 expression and cell migration/anchorage-independent growth was observed in esophageal squamous cell carcinoma cells.[10] In melanomas, CD10 protein expression level was found to be more in metastatic melanomas than primary tumors.[11] In normal thyroid tissue, its expression is not detected, but is highly expressed in follicular variants of papillary thyroid cancer.[12,13]

Clear cell renal cell carcinomas account for 65%–75% of all malignant renal tumors. The World Health Organization 2016 Classification of renal tumors has included renal cell carcinoma with leiomyomatous stroma in a category of emerging/provisional entities of renal cell carcinoma. Immunohistochemically, the tumor cells are typically positive for CD10 with cytokeratin 7.[14] These results suggest the usefulness of CD10 as a diagnostic marker of solid tumors.

Furthermore, CD10 was also identified as membrane-neutral endopeptidase-24.11, playing critical roles in the hydrolysis of biologically active peptides and their inactivation.[15] CD10 cleaves at the amino side of hydrophobic residues of several peptide hormones, including glucagon, enkephalins, substance P, neurotensin, oxytocin, and bradykinin.[16,17] In addition to its enzymatic activity, CD10

Departments of [1]Antibody Drug Development and [2]Molecular Pharmacology, Tohoku University Graduate School of Medicine, Sendai, Japan.
[3]Institute of Microbial Chemistry (BIKAKEN), Numazu, Microbial Chemistry Research Foundation, Numazu-shi, Japan.

regulates intracellular signaling pathways like PI3-kinase and Fak-Src.[18] Moreover, the association between CD10 and the tumor suppressor PTEN leads to decreased PIP3 phosphorylation, which activates the Akt pathway.[19] However, the detailed molecular functions of CD10 to promote tumor progression have not been fully investigated.

CD10 could be a useful diagnostic marker and an attractive molecular target for cancer therapy. The expression analysis along with other markers might be helpful in tumor diagnosis and treatment. Therefore, sensitive and specific monoclonal antibodies (mAbs) against CD10 are needed to diagnose and treat malignancies.

In this study, we developed a novel anti-human CD10 mAb, C_{10}Mab-31 (IgG_1, kappa), by immunizing mice with the CD10-overexpressed human renal cancer OUR-10 cells. C_{10}Mab-31 can be used in flow cytometry. We further developed the defucosylated mouse IgG_{2a} version of C_{10}Mab-31 (31-mG2a-f) and investigated the antitumor activities against CD10-overexpressed tumors.

Materials and Methods

Cell lines

P3X63Ag8U.1 (P3U1) and CHO-K1 cells were obtained from the American Type Culture Collection (ATCC; Manassas, VA). OUR-10 (a renal cancer cell line) was provided from Cell Resource Center for Biomedical Research Institute of Development, Aging and Cancer, Tohoku University (Miyagi, Japan). The pCAG-Ble vector and the pCAG-Neo vector were purchased from FUJIFILM Wako Pure Chemical Corporation (Osaka, Japan). OUR-10/CD10 and CHO/CD10 cells were established by transfecting pCAG-Ble/CD10-PAtag and pCAG-Neo/CD10-PAtag plasmids (accession no. NM_000902.3) into OUR-10 cells and CHO-K1 cells, respectively. P3U1, OUR-10, OUR-10/CD10, CHO-K1, and CHO/CD10 were cultured in RPMI 1640 medium (Nacalai Tesque, Inc., Kyoto, Japan), supplemented with 10% heat-inactivated fetal bovine serum (FBS; Thermo Fisher Scientific, Inc., Waltham, MA), 100 U/mL of penicillin, 100 μg/mL of streptomycin, and 0.25 μg/mL of amphotericin B (Nacalai Tesque, Inc.) at 37°C in a humidified atmosphere containing 5% CO_2 and 95% air.

Animals

All animal experiments were performed following relevant guidelines and regulations to minimize animal suffering and distress in the laboratory. Animal experiments for antitumor activity were approved by the Institutional Committee for Experiments of the Institute of Microbial Chemistry (permit no. 2021-019 for antibody-dependent cellular cytotoxicity [ADCC] and permit no. 2021-009 for antitumor activities). Mice were maintained in a specific pathogen-free environment (23°C ± 2°C, 55% ± 5% humidity) on an 11-hour light/13-hour dark cycle with food and water supplied *ad libitum* across the experimental period. Mice were monitored for health and weight every 2–5 days during the 3-week period of each experiment. We determined the loss of original body weight to a point >25% and/or a maximum tumor size >3000 mm^3 as humane endpoints for euthanasia. Mice were euthanized by cervical dislocation; death was verified by respiratory and cardiac arrest.

Hybridoma production

Female 4-week-old BALB/c mice were purchased from CLEA Japan (Tokyo, Japan). Animals were housed under specific pathogen-free conditions. The Animal Care and Use Committee of Tohoku University approved all the animal experiments described in this study. BALB/c mice were immunized using intraperitoneal (i.p.) injections of OUR-10/CD10 (1×10^8 cells) together with Imject Alum (Thermo Fisher Scientific, Inc.). After several additional immunizations, a booster injection was intraperitoneally administered 2 days before harvesting spleen cells. Spleen cells were then fused with P3U1 cells using PEG1500 (Roche Diagnostics, Indianapolis, IN). The resulting hybridomas were grown in RPMI 1640 medium supplemented with hypoxanthine, aminopterin, and thymidine selection medium supplement (Thermo Fisher Scientific, Inc.). Culture supernatants were screened using flow cytometry (CHO-K1 vs. CHO/CD10). MAbs were purified from the supernatants of hybridomas, cultured in Hybridoma-SFM medium (Thermo Fisher Scientific, Inc.) using Protein G Sepharose (GE Healthcare Biosciences, Pittsburgh, PA, USA).

Antibodies

To generate 31-mG_{2a}, we subcloned V_H cDNA of C_{10}Mab-31 and C_H of mouse IgG_{2a} into the pCAG-Neo vector, along with cDNA of C_{10}Mab-31 light chain into the pCAG-Zeo vector, respectively. The vector of 31-mG_{2a} was transfected into BINDS-09 cells (FUT8-knocked out ExpiCHO-S cells) using the ExpiCHO Expression System (Thermo Fisher Scientific, Inc.).[20] The resulting mAb, 31-mG_{2a}-f, was purified with Protein G Sepharose (GE Healthcare Biosciences, Pittsburgh, PA).

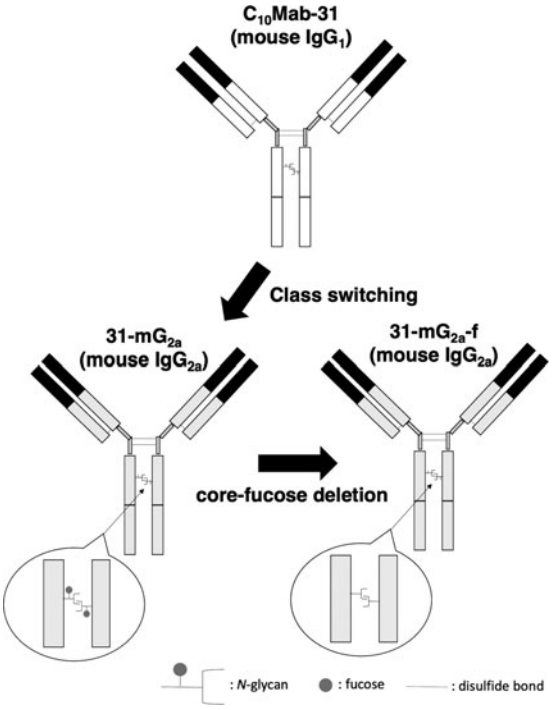

FIG. 1. Production of 31-mG_{2a} (mouse IgG_{2a}) and 31-mG_{2a}-f (defucosylated form) from an anti-CD10 mAb, C_{10}Mab-31 (mouse IgG_1).

Flow cytometry

Cells were harvested by brief exposure to 0.25% trypsin/1 mM ethylenediaminetetraacetic acid (EDTA; Nacalai Tesque, Inc.). After washing with 0.1% bovine serum albumin/phosphate-buffered saline (PBS), the cells were treated with 1 μg/mL of anti-CD10 mAbs (C_{10}Mab-31 and 31-mG_{2a}-f) for 30 minutes at 4°C and subsequently with Alexa Fluor 488-conjugated anti-mouse IgG (1:1000; Cell Signaling Technology, Inc., Danvers, MA). Fluorescence data were collected using EC800 Cell Analyzers (Sony Corp., Tokyo, Japan).

ADCC

Six 6-week-old female BALB/c nude mice were purchased from Charles River, spleens were removed aseptically, and single-cell suspensions were obtained by dispersing the spleens using a syringe and pressing through stainless steel mesh. Erythrocytes were effectively lysed by a 10-second exposure to ice-cold distilled water. Splenocytes were washed with Dulbecco's modified Eagle's medium (DMEM) and resuspended in DMEM with 10% FBS as effector cells. Target cells were labeled with 10 μg/mL calcein AM (Thermo Fisher Scientific, Inc.) and resuspended in the medium. The target cells (2×10^4 cells/well) were placed in 96-well plates and mixed with effector cells and either 31-mG_{2a}-f or control IgG (mouse IgG_{2a}) (Sigma-Aldrich Corp., St. Louis, MO).

After a 5-hour incubation period, the calcein release of supernatant from each well was measured. The fluorescence intensity was determined at an excitation wavelength of 485 nm and an emission wavelength of 538 nm using a microplate reader (Power Scan HT) (BioTek Instruments, Winooski, VT). Cytolytic activity (as % of lysis) was calculated using the following formula: % lysis $= (E - S)/(M - S) \times 100$ (where E is the fluorescence released in the experimental cultures of target and effector cells, S is the spontaneous

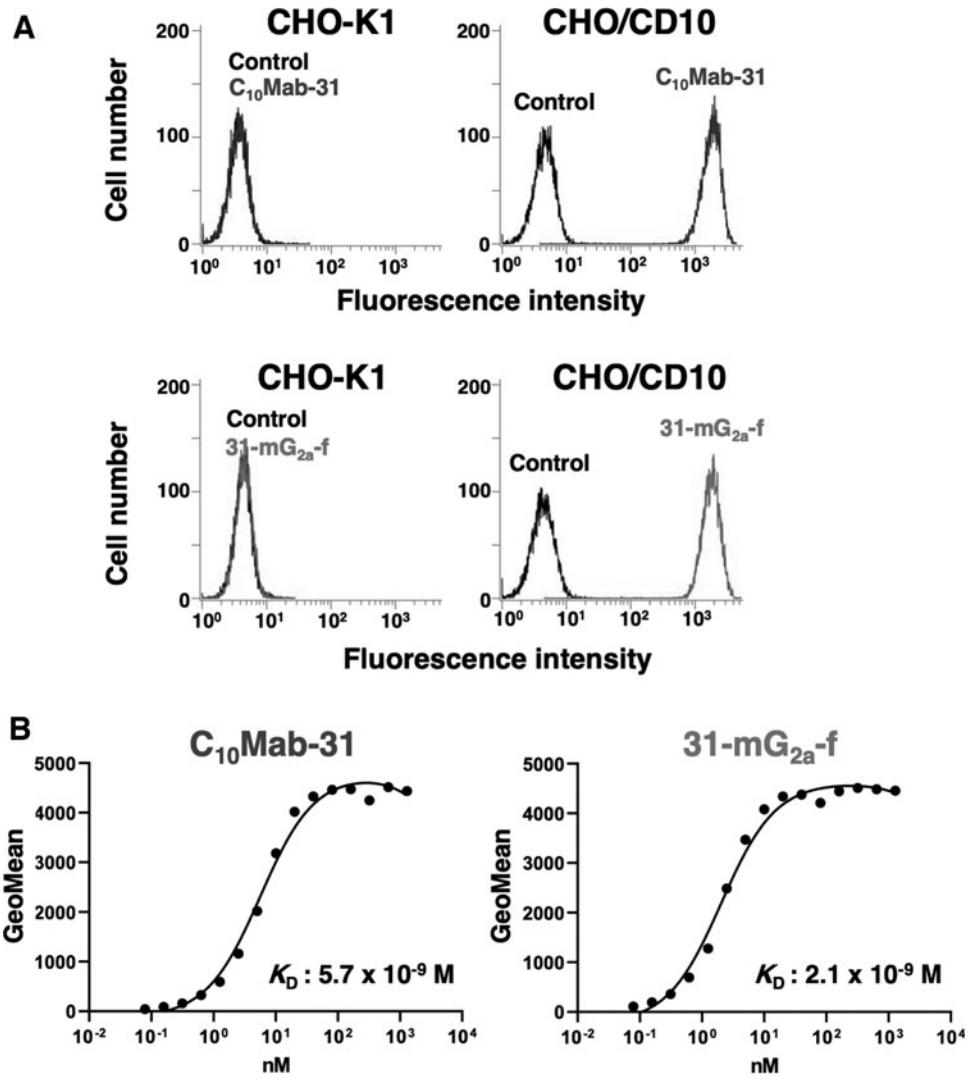

FIG. 2. Flow cytometry using C_{10}Mab-31 and 31-mG_{2a}-f. **(A)** CHO-K1 and CHO/CD10 cells were treated with C_{10}Mab-31 and 31-mG_{2a}-f, or buffer control, followed by secondary antibodies. **(B)** Determination of the binding affinity of C_{10}Mab-31 and 31-mG_{2a}-f for CHO/CD10 cells using flow cytometry. CHO/CD10 cells were suspended in 100 µL of serially diluted C_{10}Mab-31 and 31-mG_{2a}-f, followed by the addition of Alexa Fluor 488-conjugated anti-mouse IgG. Fluorescence data were collected using the EC800 Cell Analyzer.

fluorescence released in cultures containing only target cells, and *M* is the maximum fluorescence obtained by adding a lysis buffer containing 0.5% Triton X-100, 10 mM Tris-HCl (pH 7.4), and 10 mM of EDTA to the target cells to lyse all cells).

Complement-dependent cytotoxicity (CDC)

CHO/CD10 cells were placed in 96-well plates of 2×10^4 cells/well in DMEM supplemented with 10% FBS. Cells were incubated with either 31-mG_{2a}-f or the control IgG (mouse IgG_{2a}) (Sigma-Aldrich Corp.) and 10% of rabbit complement (Low-Tox-M Rabbit Complement) (Cedarlane Laboratories, Hornby, ON, Canada) for 5 hours at 37°C. To assess cell viability, MTS [3-(4,5-dimethylthiazol-2-yl)-5-(3-carboxymethoxyphenyl)-2-(4-sulfophenyl)-2H-tetrazolium; inner salt] assay was performed using a CellTiter 96 AQueous assay kit (Promega, Madison, WI).

Antitumor activity of 31-mG_{2a}-f

Female BALB/c nude mice (6-week old) were purchased from Charles River (Kanagawa, Japan) and used in experiments when they were 6 weeks old. CHO/CD10 (0.3 mL of 1.33×10^8/mL in DMEM) was mixed with 0.5 mL of BD Matrigel Matrix Growth Factor Reduced (BD Biosciences, San Jose, CA). A 100 μL suspension (containing 5×10^6 cells) was injected subcutaneously into the left flanks of nude mice. After day 6, 100 μg of 31-mG_{2a}-f and control mouse IgG (Sigma-Aldrich Corp.) in 100 μL PBS were injected into the peritoneal cavity of each mouse. Additional antibodies were then injected on days 14 and 21. The tumor diameter and volume were determined as previously described.[21] The mice were euthanized 25 days after cell implantation. All data were expressed as mean ± standard error of the mean (SEM).

Statistical analyses

All data are expressed as mean ± SEM. Statistical analysis was conducted with Welch's *t* test for ADCC, CDC, and tumor weight. Analysis of variance (ANOVA) and Sidak's multiple comparisons tests were conducted for tumor volume and mouse weight. All calculations were performed using GraphPad Prism 8. A *p*-value of <0.05 was considered statistically significant.

Results

Flow cytometry analysis against CHO/CD10 cells using anti-CD10 mAbs

In this study, we immunized one mouse with OUR-10/CD10 cells. Flow cytometry was conducted to check reactions with CHO-K1 and CD10-overexpressed CHO-K1 (CHO/CD10) cells. A stronger reaction against CHO/CD10 was needed compared with CHO-K1. We obtained one clone, C_{10}Mab-31, of the IgG_1 subclass. We converted the subclass of C_{10}Mab-31 into mouse IgG_{2a} to add ADCC and CDC activities. Furthermore, we produced a defucosylated anti-CD10 mAb (31-mG_{2a}-f) using BINDS-09 cells (FUT8-deficient ExpiCHO-S cells). This process is summarized in Figure 1.

We first characterized anti-CD10 mAbs in flow cytometry. Both C_{10}Mab-31 and 31-mG_{2a}-f reacted with CHO/CD10 cells, not with CHO-K1 cells, indicating that C_{10}Mab-31 and 31-mG_{2a}-f are specific for CD10 (Fig. 2A).

Kinetic analysis of C_{10}Mab-31 and 31-mG_{2a}-f interactions with CHO/CD10 cells was conducted by flow cytometry. As shown in Figure 2B, the K_D for C_{10}Mab-31 and 31-mG_{2a}-f interactions with CHO/CD10 cells was 5.7×10^{-9} M and 2.1×10^{-9} M, respectively, suggesting that both C_{10}Mab-31 and 31-mG_{2a}-f showed a high affinity for CHO/CD10 cells.

31-mG_{2a}-f-mediated ADCC and CDC in CHO/CD10 cells

We investigated whether 31-mG_{2a}-f was capable of mediating ADCC against CHO/CD10 cells. As shown in Figure 3, 31-mG_{2a}-f showed ADCC (21.4% cytotoxicity) against CHO/CD10 cells more effectively than the control mouse IgG_{2a} (9.9% cytotoxicity; $p < 0.05$).

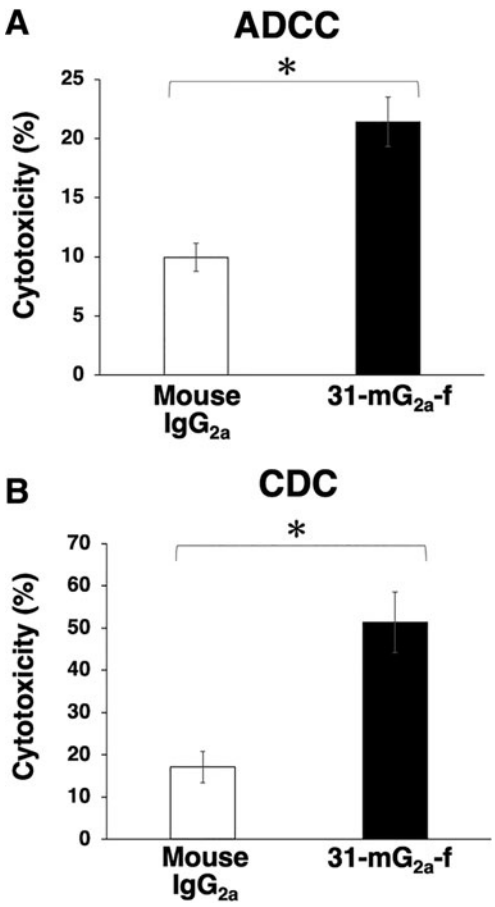

FIG. 3. Evaluation of ADCC and CDC elicited by 31-mG_{2a}-f. **(A)** ADCC elicited by 31-mG_{2a}-f, control mouse IgG_{2a} targeting CHO/CD10 cells. **(B)** CDC elicited by 31-mG_{2a}-f, control mouse IgG_{2a} targeting CHO/CD10 cells. Values are mean ± SEM. Asterisks indicate statistical significance (*$p < 0.05$; Welch's *t*-test). ADCC, antibody-dependent cellular cytotoxicity; CDC, complement-dependent cytotoxicity; SEM, standard error of the mean.

We then investigated whether 31-mG_{2a}-f could mediate CDC against CHO/CD10 cells. As shown in Figure 3, 31-mG_{2a}-f elicited a higher degree of CDC (51.3% cytotoxicity) in CHO/CD10 cells compared with that elicited by control mouse IgG_{2a} (17.1% cytotoxicity; $p < 0.05$). These results demonstrated that 31-mG_{2a}-f promoted significantly higher levels of ADCC and CDC against CHO/CD10 cells.

31-mG_{2a}-f-mediated antitumor activities against the CHO/CD10 xenograft model

To study the antitumor activity of 31-mG_{2a}-f on cell growth *in vivo*, CHO/CD10 cells were subcutaneously implanted into the flanks of nude mice. 31-mG_{2a}-f and control mouse IgG were injected three times (on days 6, 14, and 21

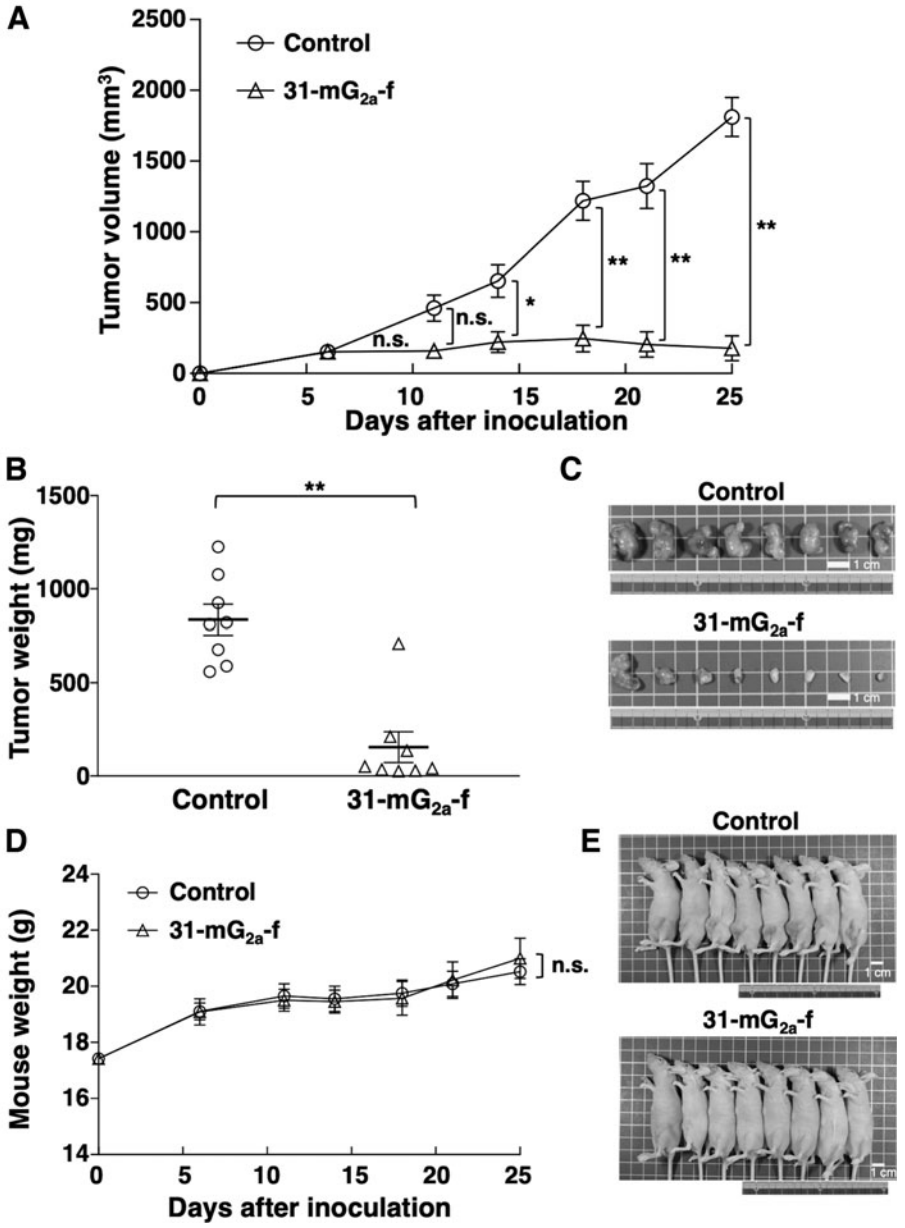

FIG. 4. Evaluation of antitumor activity of 31-mG_{2a}-f in CHO/CD10 xenografts. **(A)** CHO/CD10 cells (5×10^6 cells) were injected subcutaneously into the left flank. After day 6, 100 μg of 31-mG_{2a}-f or control mouse IgG in 100 μl PBS were injected intraperitoneally into mice; additional antibodies were then injected on days 14 and 21. The tumor volume was measured on days 6, 11, 14, 18, 21, and 25 after the injection. Value are means ± SEM. Asterisks indicate statistical significance (*$p < 0.05$, **$p < 0.01$; ANOVA and Sidak's multiple comparisons test). **(B)** Tumors of CHO/CD10 xenografts were resected from 31-mG_{2a}-f and control mouse IgG groups. Tumor weight on day 25 was measured from excised xenografts. Values are mean ± SEM. Asterisk indicates statistical significance (**$p < 0.01$, Welch's *t*-test). **(C)** Resected tumors of CHO/CD10 xenografts from the control mouse IgG and 31-mG_{2a}-f groups on day 25. Scale bar, 1 cm. **(D)** Body weights and appearance of the mice implanted with CHO/CD10 xenografts. Body weights of mice implanted with CHO/CD10 xenografts were recorded on days 6, 11, 14, 18, 21, and 25. (n.s., ANOVA and Sidak's multiple comparisons test). **(E)** Body appearance of mice on day 25. Scale bar, 1 cm. ANOVA, analysis of variance; n.s., not significant; PBS, phosphate-buffered saline.

after cell injections) into the peritoneal cavity of mice. Tumor formation was observed in mice from the control and 31-mG_{2a}-f-treated groups in CHO/CD10 xenograft models. 31-mG_{2a}-f significantly reduced the tumor development of CHO/CD10 xenograft compared with that in control mouse IgG on days 14 ($p<0.05$), 18 ($p<0.01$), 21 ($p<0.01$), and 25 ($p<0.01$) (Fig. 4A). The administration of 31-mG_{2a}-f resulted in a 90% reduction of tumor volume compared with that of the control mouse IgG on day 25 postinjection.

The tumor weight of mice treated with 31-mG_{2a}-f was significantly lower than that in the control mouse IgG group in CHO/CD10 xenograft models (82% reduction; $p<0.01$, Fig. 4B). The resected tumors of CHO/CD10 xenografts are depicted in Figure 4C. Body weight was not significantly different among the two groups in CHO/CD10 xenograft models (Fig. 4D). CHO/CD10 xenograft mice models on day 25 are shown in Figure 4E.

Taken together, these results indicate that the administration of 31-mG_{2a}-f effectively reduced the growth of CHO/CD10 xenografts.

Discussion

MAbs to target solid tumor antigens have been extensively explored.[22] Among the U.S. Food and Drug Administration-approved mAbs, most mAbs receiving approval in solid tumors have targeted two members of the ERBB family, EGFR or HER2.[23] In addition, the cytotoxic agent conjugated mAbs against HER2,[24–26] Nectin-4,[27] and TROP2,[28,29] have been approved by FDA in solid tumors. Nonconjugated mAbs can exhibit several different mechanisms of action, including ADCC and CDC activities, while conjugated mAbs rely on the direct cytotoxicity of their payloads through endocytosis of receptor-bound mAbs-drug conjugates.

This study showed that anti-CD10 mAb, 31-mG_{2a}-f, exhibits ADCC and CDC activities and potent antitumor activity in CHO/CD10 xenografts. Also, a 90% reduction in tumor volume and 82% reduction in tumor weight were achieved (Fig. 4). These therapeutic outcomes depend on the isotype and specific nature of the mAb (i.e., specific binding epitope, affinity of target binding, and particular conformation), as well as the nature of the target antigen. We have not determined the binding epitope; however, both C_{10}Mab-31 and 31-mG_{2a}-f showed high affinity to target (Fig. 2B), and the defucosylation in 31-mG_{2a}-f confers high ADCC activity. These results expect the use of anti-CD10 mAb not only for pathological diagnosis but also for tumor therapy.

On the other hand, an important consideration in tumor-targeted antibody-drug is the distribution of the target protein expression in normal tissues, which has important implications for off-target effects. Previously, we established cancer-specific monoclonal antibodies (CasMabs) technology against cell surface proteins and developed some CasMabs, including anti-podoplanin mAb (LpMab-2)[30] and anti-podocalyxin (PcMab-60).[31] For example, LpMab-2 can recognize both a Thr55-Leu64 peptide of human podoplanin and cancer-type aberrant glycosylation of Thr55 and/or Ser56, unexpressed in normal cells.[30] Therefore, the establishment of CasMabs to CD10 is essential to reduce the side effects.

CD10 belongs to the mammalian neutral endopeptidases and has a C-terminal extracellular domain that contains the active site.[5,16,17] The X-ray crystal structure of the extracellular domain (52–749 aa) of CD10 was solved with a metalloproteinase inhibitor phosphoramidon. The structure reveals the important consensus sequences HExxH and ExxxD that embrace a large central cavity, including the active site. The inhibitor is bound to this cavity, which provides detailed ligand recognition.[32] However, there is no information about the epitope of C_{10}Mab-31. Therefore, further studies are warranted for determining the epitope. We have developed two novel epitope mapping methods, such as REMAP and HisMAP method, and determined the epitope of anti-EGFR mAbs (EMab-51 and EMab-134),[33,34] an anti-CD44 mAb (C_{44}Mab-46),[35] and an anti-CD20 mAb (C_{20}Mab-60).[36] Furthermore, based on the epitope analysis, the investigations of C_{10}Mab-31 effects on the CD10-mediated ligand recognition and endopeptidase activity are thought to be required.

Recently, the functional anti-CD10 mAb (JMAM-1) has been reported.[37] JMAM-1 has a cytostatic effect on mesothelioma MSTO-211H cells *in vitro* and exhibits a prolonged survival of NCI-H226 tumor-bearing mice. However, the detailed mechanism of the antitumor effect has not been investigated. Moreover, CD10-positive subpopulation in head and neck squamous cell carcinoma possesses cancer stem cell-like properties and expresses a high level of stem cell marker OCT3/4. The elevated level of OCT3/4 in CD10-positive cells results in the promotion of stemness and tumor formation, which implies therapeutic resistance and refractory.[38] Therefore, the functional investigations of C_{10}Mab-31 (or 31-mG_{2a}-f) in endogenous CD10-expressing tumor cells are required to understand the antitumor activity of 31-mG_{2a}-f.

Author Disclosure Statement

No competing financial interests exist.

Funding Information

This research was supported, in part, by Japan Agency for Medical Research and Development (AMED) under grant nos. JP22ama121008 (to Y.K.), JP21am0401013 (to Y.K.), and JP21am0101078 (to Y.K.). and by the Japan Society for the Promotion of Science (JSPS) Grants-in-Aid for Scientific Research (KAKENHI) under grant nos. 21K07168 (to M.K.K.) and 19K07705 (to Y.K.).

References

1. Borella L, Sen L, and Casper JT: Acute lymphoblastic leukemia (ALL) antigens detected with antisera to E rosette-froming and non-E rosette-forming ALL blasts. J Immunol 1977;118:309–315.
2. Billing R, Minowada J, Cline M, Clark B, and Lee K: Acute lymphocytic leukemia-associated cell membrane antigen. J Natl Cancer Inst 1978;61:423–429.
3. Minowada J, Janossy G, Greaves MF, Tsubota T, Srivastava BI, Morikawa S, and Tatsumi E: Expression of an antigen associated with acute lymphoblastic leukemia in human leukemia-lymphoma cell lines. J Natl Cancer Inst 1978;60:1269–1277.
4. Béné MC: Immunophenotyping of acute leukaemias. Immunol Lett 2005;98:9–21.

5. Erdös EG, and Skidgel RA: Neutral endopeptidase 24.11 (enkephalinase) and related regulators of peptide hormones. FASEB J 1989;3:145–151.
6. Freedman A: Follicular lymphoma: 2018 update on diagnosis and management. Am J Hematol 2018;93:296–305.
7. Cortelazzo S, Ponzoni M, Ferreri AJ, and Hoelzer D: Lymphoblastic lymphoma. Crit Rev Oncol Hematol 2011; 79:330–343.
8. Mishra D, Singh S, and Narayan G: Role of B cell development marker CD10 in cancer progression and prognosis. Mol Biol Int 2016;2016:4328697.
9. Iwase T, Kushima R, Mukaisho K, Mitsufuji S, Okanoue T, and Hattori T: Overexpression of CD10 and reduced MUC2 expression correlate with the development and progression of colorectal neoplasms. Pathol Res Pract 2005;201: 83–91.
10. Lee KW, Sung CO, Kim JH, Kang M, Yoo HY, Kim HH, Um SH, and Kim SH: CD10 expression is enhanced by Twist1 and associated with poor prognosis in esophageal squamous cell carcinoma with facilitating tumorigenicity *in vitro* and *in vivo*. Int J Cancer 2015;136: 310–321.
11. Bilalovic N, Sandstad B, Golouh R, Nesland JM, Selak I, and Torlakovic EE: CD10 protein expression in tumor and stromal cells of malignant melanoma is associated with tumor progression. Mod Pathol 2004;17:1251–1258.
12. Mokhtari M, and Ameri F: Diagnostic value of CD-10 marker in differentiating of papillary thyroid carcinoma from benign thyroid lesions. Adv Biomed Res 2014;3:206.
13. Tomoda C, Kushima R, Takeuti E, Mukaisho K, Hattori T, and Kitano H: CD10 expression is useful in the diagnosis of follicular carcinoma and follicular variant of papillary thyroid carcinoma. Thyroid 2003;13:291–295.
14. Yeh YA, Constantinescu M, Chaudoir C, Tanner A, Serkin F, Yu X, Fazili T, and Lurie AA: Renal cell carcinoma with leiomyomatous stroma: A review of an emerging entity distinct from clear cell conventional renal cell carcinoma. Am J Clin Exp Urol 2019;7:321–326.
15. Kenny AJ, O'Hare MJ, and Gusterson BA: Cell-surface peptidases as modulators of growth and differentiation. Lancet 1989;2:785–787.
16. Roques BP, Noble F, Daugé V, Fournié-Zaluski MC, and Beaumont A: Neutral endopeptidase 24.11: Structure, inhibition, and experimental and clinical pharmacology. Pharmacol Rev 1993;45:87–146.
17. Turner AJ, and Tanzawa K: Mammalian membrane metallopeptidases: NEP, ECE, KELL, and PEX. FASEB J 1997;11:355–364.
18. Maguer-Satta V, Besançon R, and Bachelard-Cascales E: Concise review: Neutral endopeptidase (CD10): A multifaceted environment actor in stem cells, physiological mechanisms, and cancer. Stem Cells 2011;29:389–396.
19. Sumitomo M, Shen R, and Nanus DM: Involvement of neutral endopeptidase in neoplastic progression. Biochim Biophys Acta 2005;1751:52–59.
20. Takei J, Kaneko MK, Ohishi T, Hosono H, Nakamura T, Yanaka M, Sano M, Asano T, Sayama Y, Kawada M, Harada H, and Kato Y: A defucosylated anti-CD44 monoclonal antibody 5-mG2a-f exerts antitumor effects in mouse xenograft models of oral squamous cell carcinoma. Oncol Rep 2020;44:1949–1960.
21. Hosono H, Takei J, Ohishi T, Sano M, Asano T, Sayama Y, Nakamura T, Yanaka M, Kawada M, Harada H, Kaneko MK, and Kato Y: Anti-EGFR monoclonal antibody 134-mG2a exerts antitumor effects in mouse xenograft models of oral squamous cell carcinoma. Int J Mol Med 2020;46: 1443–1452.
22. Tsao LC, Force J, and Hartman ZC: Mechanisms of therapeutic antitumor monoclonal antibodies. Cancer Res 2021; 81:4641–4651.
23. Zahavi D, and Weiner L: Monoclonal antibodies in cancer therapy. Antibodies (Basel) 2020;9:34.
24. Li BT, Smit EF, Goto Y, Nakagawa K, Udagawa H, Mazières J, Nagasaka M, Bazhenova L, Saltos AN, Felip E, Pacheco JM, Pérol M, Paz-Ares L, Saxena K, Shiga R, Cheng Y, Acharyya S, Vitazka P, Shahidi J, Planchard D, and Jänne PA: Trastuzumab deruxtecan in HER2-mutant non-small-cell lung cancer. N Engl J Med 2022;386:241–251.
25. Modi S, Saura C, Yamashita T, Park YH, Kim SB, Tamura K, Andre F, Iwata H, Ito Y, Tsurutani J, Sohn J, Denduluri N, Perrin C, Aogi K, Tokunaga E, Im SA, Lee KS, Hurvitz SA, Cortes J, Lee C, Chen S, Zhang L, Shahidi J, Yver A, and Krop I: Trastuzumab deruxtecan in previously treated HER2-positive breast cancer. N Engl J Med 2020;382:610–621.
26. Shitara K, Bang YJ, Iwasa S, Sugimoto N, Ryu MH, Sakai D, Chung HC, Kawakami H, Yabusaki H, Lee J, Saito K, Kawaguchi Y, Kamio T, Kojima A, Sugihara M, and Yamaguchi K: Trastuzumab deruxtecan in previously treated HER2-positive gastric cancer. N Engl J Med 2020;382: 2419–2430.
27. Heath EI, and Rosenberg JE: The biology and rationale of targeting nectin-4 in urothelial carcinoma. Nat Rev Urol 2021;18:93–103.
28. Bardia A, Hurvitz SA, Tolaney SM, Loirat D, Punie K, Oliveira M, Brufsky A, Sardesai SD, Kalinsky K, Zelnak AB, Weaver R, Traina T, Dalenc F, Aftimos P, Lynce F, Diab S, Cortés J, O'Shaughnessy J, Diéras V, Ferrario C, Schmid P, Carey LA, Gianni L, Piccart MJ, Loibl S, Goldenberg DM, Hong Q, Olivo MS, Itri LM, and Rugo HS: Sacituzumab govitecan in metastatic triple-negative breast cancer. N Engl J Med 2021;384: 1529–1541.
29. Goldenberg DM, Stein R, and Sharkey RM: The emergence of trophoblast cell-surface antigen 2 (TROP-2) as a novel cancer target. Oncotarget 2018;9:28989–29006.
30. Kato Y, and Kaneko MK: A cancer-specific monoclonal antibody recognizes the aberrantly glycosylated podoplanin. Sci Rep 2014;4:5924.
31. Kaneko MK, Ohishi T, Kawada M, and Kato Y: A cancer-specific anti-podocalyxin monoclonal antibody (60-mG(2a)-f) exerts antitumor effects in mouse xenograft models of pancreatic carcinoma. Biochem Biophys Rep 2020;24: 100826.
32. Oefner C, D'Arcy A, Hennig M, Winkler FK, and Dale GE: Structure of human neutral endopeptidase (Neprilysin) complexed with phosphoramidon. J Mol Biol 2000;296: 341–349.
33. Sano M, Kaneko MK, Aasano T, and Kato Y: Epitope mapping of an antihuman EGFR monoclonal antibody (EMab-134) using the REMAP method. Monoclon Antib Immunodiagn Immunother 2021;40:191–195.
34. Nanamiya R, Sano M, Asano T, Yanaka M, Nakamura T, Saito M, Tanaka T, Hosono H, Tateyama N, Kaneko MK, and Kato Y: Epitope mapping of an anti-human epidermal

growth factor receptor monoclonal antibody (EMab-51) using the RIEDL insertion for epitope mapping method. Monoclon Antib Immunodiagn Immunother 2021;40:149–155.
35. Asano T, Kaneko MK, Takei J, Tateyama N, and Kato Y: Epitope mapping of the anti-CD44 monoclonal antibody (C44Mab-46) using the REMAP method. Monoclon Antib Immunodiagn Immunother 2021;40:156–161.
36. Asano T, Takei J, Furusawa Y, Saito M, Suzuki H, Kaneko MK, and Kato Y: Epitope mapping of an anti-CD20 monoclonal antibody (C20Mab-60) using the His-MAP method. Monoclon Antib Immunodiagn Immunother 2021;40:243–249.
37. Mizutani N, Abe M, Kajino K, and Matsuoka S: A new CD10 antibody inhibits the growth of malignant mesothelioma. Monoclon Antib Immunodiagn Immunother 2021; 40:21–27.
38. Fukusumi T, Ishii H, Konno M, Yasui T, Nakahara S, Takenaka Y, Yamamoto Y, Nishikawa S, Kano Y, Ogawa H, Hasegawa S, Hamabe A, Haraguchi N, Doki Y, Mori M, and Inohara H: CD10 as a novel marker of therapeutic resistance and cancer stem cells in head and neck squamous cell carcinoma. Br J Cancer 2014;111:506–514.

Address correspondence to:
Yukinari Kato
Department of Molecular Pharmacology
Tohoku University Graduate School of Medicine
2-1, Seiryo-machi, Aoba-ku
Sendai 980-8575
Japan

E-mail: yukinarikato@med.tohoku.ac.jp

Received: September 27, 2021
Accepted: February 14, 2022